

PAPER • OPEN ACCESS

## Structural, electrical and magnetic study of manganites $\text{Pr}_{0.6}\text{Sr}_{0.4}\text{MnO}_3$ thin films

To cite this article: D S Neznakhin *et al* 2016 *J. Phys.: Conf. Ser.* **690** 012002

View the [article online](#) for updates and enhancements.

### Related content

- [Magnetic transition behavior of perovskite manganites  \$\text{Nd}\_{0.5}\text{Sr}\_{0.3}\text{Ca}\_{0.2}\text{MnO}\_3\$  polycrystalline](#)  
Ru Xing, Su-Lei Wan, Wen-Qing Wang *et al.*
- [Magnetic and critical properties of  \$\text{Pr}\_{0.6}\text{Sr}\_{0.4}\text{MnO}\_3\$  nanocrystals prepared by a combination of the solid state reaction and the mechanical ball milling methods](#)  
Nguyen Thi Dung, Dinh Chi Linh, Pham Duc Huyen Yen *et al.*

### Recent citations

- [Surface and structural analysis of epitaxial  \$\text{La}\_{1-x}\text{Sr}\_x\(\text{Mn}\_{1-y}\text{Co}\_y\)\_z\text{O}\_3\$  films](#)  
Saulius Kaciulis *et al*



**IOP | ebooks™**

Bringing together innovative digital publishing with leading authors from the global scientific community.

Start exploring the collection—download the first chapter of every title for free.

# Structural, electrical and magnetic study of manganites $\text{Pr}_{0.6}\text{Sr}_{0.4}\text{MnO}_3$ thin films

D S Neznakhin<sup>1</sup>, Yu E Samoshkina<sup>2</sup>, M S Molokeev<sup>2</sup> and S V Semenov<sup>2</sup>

<sup>1</sup>Ural Federal University, Ekaterinburg 620000, Russia

<sup>2</sup>L.V. Kirensky Institute of Physics SB RAS, 660036 Krasnoyarsk, Russia

E-mail: d.s.neznakhin@urfu.ru

**Abstract.** Thin polycrystalline  $\text{Pr}_{0.6}\text{Sr}_{0.4}\text{MnO}_3$  films were grown on the Y stabilized zirconium oxide substrates by magnetron sputtering using RF power and off-axis sputtering scheme with double cathodes. Only one polycrystalline phase with structural parameters consistent with that for the corresponding bulk sample was revealed in the films. Electric resistivity dependence on temperature demonstrates the shape characteristic for the substances with the Mott transition. The difference between magnetization temperature curves measured in the zero field cooling and field cooling modes was revealed. Magnetization field dependences were presented by the hysteresis loops changing their form with temperature.

## I. Introduction

Substituted manganites with the perovskite structure and general formulae  $\text{R}_{1-x}\text{A}_x\text{MnO}_3$  (where R is a trivalent lanthanide and A is a divalent alkaline earth metal) has attracted great attention in the past few decades [1-6]. The parent compounds  $\text{RMnO}_3$  are known to be the Mott insulator with the antiferromagnetic ground state (AFM). At the partial replacement of the lanthanide ions with the divalent alkaline earth, a great variety of magnetic and electric phases appears in dependence on the divalent ion type and its concentration. In particular, for the region of  $x$  meanings from  $\sim 0.2$  to  $\sim 0.5$ , the metallic ferromagnetic phase is usually realized.

Historically, the  $\text{La}_{1-x}\text{Sr}_x\text{MnO}_3$  compounds were the main objects of investigation among manganites doped with Sr. As concerns Pr-Sr manganites, only a few works devoted to the magnetic and transport properties of the single- and polycrystalline bulk samples are available in literature [7-13]. Recently, we have investigated, for the first time, the visible magnetic circular dichroism (MCD) in  $\text{Pr}_{1-x}\text{Sr}_x\text{MnO}_3$  thin films and have revealed remarkably different temperature dependences of the MCD maxima intensity at different wave lengths in the case of  $\text{Pr}_{0.6}\text{Sr}_{0.4}\text{MnO}_3$  [14]. In this connection, a detailed investigation of electric and magnetic properties for the same samples seems to be of primary importance.

The aim of the present paper is a study of the temperature and field dependences of the electric resistivity and magnetization of the  $\text{Pr}_{0.6}\text{Sr}_{0.4}\text{MnO}_3$  polycrystalline films in wide intervals of temperature and external magnetic field.

## 2. Experimental setup and samples

Films of different thicknesses (20, 30, 50, 80, and 130 nm) were prepared by the dc magnetron sputtering technique analogously to that presented in [15]. The single-phased  $\text{Pr}_{0.6}\text{Sr}_{0.4}\text{MnO}_3$  targets were obtained by solid-state synthesis using stoichiometric  $\text{Pr}_2\text{O}_3$ , SrO, and  $\text{MnO}_2$  powders as the



starting materials. The residual gas pressure in the vacuum chamber was  $3 \times 10^{-6}$  Torr. The operating total pressure of the Ar and O<sub>2</sub> gas mixture (with a ratio of 4:1) was  $3 \times 10^{-3}$  Torr. The films were grown onto yttrium stabilized zirconium (YSZ) oxide (311) substrates which temperature during the sputtering was 750°C.

The crystal structure and phase purity of the samples were examined by the powder X-ray diffraction (XRD) with CuK $\alpha$  radiation. The electric conductivity dependence on temperature and external magnetic field was investigated using the standard four-point probe technique in the temperature interval 78–300 K. Magnetic measurements were carried out with a Quantum Design MPMS-XL7 EC superconducting-quantum interference device (SQUID) magnetometer in the temperature range of 5–300 K and in magnetic fields up to 20 kOe applied parallel and perpendicular to the films plane.

### 3. Results and discussion

XRD pattern for the synthesized films shows large peaks corresponding to the YSZ substrate and series of relatively narrow peaks with small intensities corresponding to only one polycrystalline phase Pr<sub>0.6</sub>Sr<sub>0.4</sub>MnO<sub>3</sub> without pronounced texture (figure 1). The crystal structure was refined within the orthorhombic Pnma space group with the lattice parameters and the average crystallites size presented in Table 1. Structural parameters of the studied films are consistent with the structural data for the bulk polycrystalline Pr<sub>0.6</sub>Sr<sub>0.4</sub>MnO<sub>3</sub> samples presented, for example, in Ref. [16] and also shown in Table 1.

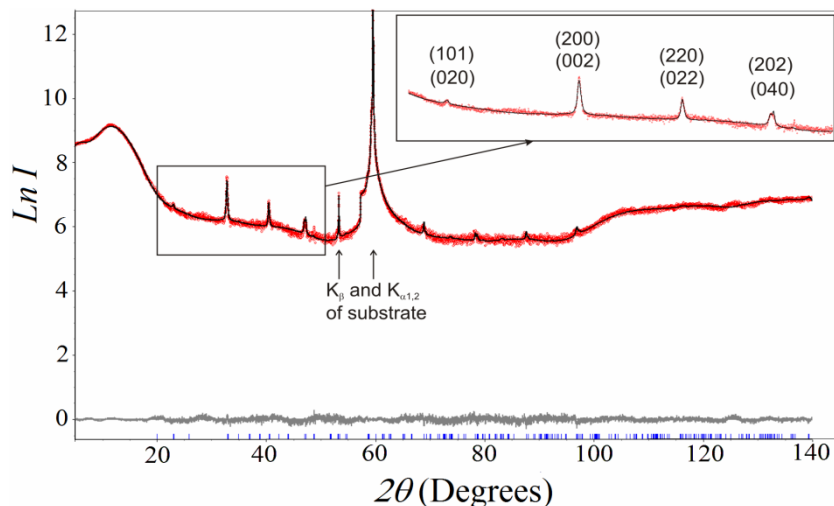


**Figure 1.** Room temperature XRD pattern for the Pr<sub>0.6</sub>Sr<sub>0.4</sub>MnO<sub>3</sub> film of 130 nm in thickness. The reflections from the substrate are indicated by arrows.

The temperature dependences of electric resistivity,  $R(T)$ , measured in the temperature interval 78–300 K both without magnetic field and under the magnetic field of 15 kOe are shown in figure 2 for the thickest film (130 nm). For the films of other thicknesses the pictures are similar. The  $R(T)$  curves show a single semiconductor-metal (called usually as insulator-metallic) transition at  $T_R$ , which is associated, in the case of manganites, with the competition between the double exchange and the super exchange interactions [16]. The resistivity value is seen to decrease in magnetic field, and  $T_R$  shifts to higher temperatures. Just the same  $R(T)$  and  $T_R(H)$  behavior was observed in Ref. [16] for the polycrystalline bulk Pr<sub>0.6</sub>Sr<sub>0.4</sub>MnO<sub>3</sub> samples with the only difference: the  $T_R$  value in our case is distinctly lower. The magnetic field effect on the  $R$  and  $T_R$  behavior was explained in Ref. [17] by the fact that the applied magnetic field delocalizes the charge carriers suppressing the resistivity causing the local ordering of the electron spins. Due to the ordering, ferromagnetic metallic state may suppress the higher temperature paramagnetic state resulting in an increase of  $T_R$  value under the influence of

magnetic field. Usually,  $T_R$  coincides with  $T_C$ — temperature of the magnetic ordering, while in our case and also in Ref. [16]  $T_R$  is essentially lower as compared to  $T_C$ . It is possible to assume that the contribution of the inter-grain spin-polarized tunneling across the grain boundaries causes the  $T_R$  value lowering. The thin film geometry may affect the  $R$  value and temperature behavior too. This question needs further study.

**Table 1.** Structural parameters of the  $\text{Pr}_{0.6}\text{Sr}_{0.4}\text{MnO}_3$  film of 130 nm in thickness.

Parameters	$\text{Pr}_{0.6}\text{Sr}_{0.4}\text{MnO}_3$ Our data	$\text{Pr}_{0.6}\text{Sr}_{0.4}\text{MnO}_3$ Ref. [16]
$a$ (Å)	5.4465(7)	5.4805
$b$ (Å)	7.721(1)	7.6726
$c$ (Å)	5.422(1)	5.4401
$V$ (Å <sup>3</sup> )	228.00(6)	228.75
Average crystallites size (nm)	45 (7) along $b$ axis 62 (3) along $a$ and $c$ axes	10.95

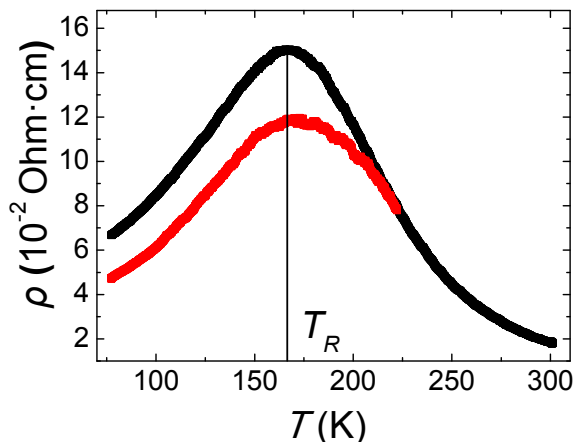


**Figure 2.** Temperature dependences of the resistivity in zero (black curve) and 15 kOe (red curve) magnetic field for the  $\text{Pr}_{0.6}\text{Sr}_{0.4}\text{MnO}_3$  film of 130 nm in thickness.

The magnetization temperature dependences,  $M(T)$ , are shown in figure3 for the film with a thickness of 80 nm. The dependences were obtained for field cooling (FC) and zero field cooling (ZFC) modes at different values and orientations of the external magnetic field. In the FC procedure, the magnetization magnitude was measured at a cooling and heating of samples at the same magnetic field.

Consider first the FC process: for all  $H$  values and orientations, smooth curves are observed with an increase in the magnetization with lowering temperature. Just below  $T_C$ , the increase is not as sharp as in the case of bulk polycrystalline samples [9, 10]. Besides, the features at 100K and the temperature hysteresis observed in [10] are not revealed here. Note that such features were also not observed for stoichiometric  $\text{Pr}_{0.6}\text{Sr}_{0.4}\text{MnO}_3$  polycrystals by some other authors [13]. The  $T_C$  value is approximately equal to 250 K, that is notably lower than the  $T_C$  value for the bulk polycrystalline samples (310 K) [10].

The FC and ZFC curves diverge from each other at some temperature  $T_{irr}$ , and then the ZFC curve runs below the FC curve demonstrating a broad maximum at a certain temperature  $T_m$ . At that, the ZFC magnetization diminishes with lowering temperature, sometimes, almost to zero. Such a behavior is typical for heterogeneous magnetic samples such as ensembles of superparamagnetic particles, or spin glasses, or polycrystalline samples with the random distribution of the easy magnetization axes of the crystallites. The temperatures  $T_{irr}$  and  $T_m$  as well as the ZFC maximum width depend on the magnitude and orientation of the external magnetic field. As it was mentioned above, the films investigated consist of randomly oriented nanocrystals. At the cooling of the films in a magnetic field,

the magnetization direction in each crystallite is determined by the competition between the crystallographic anisotropy energy and the Zeeman energy.

For sufficiently large values of the external magnetic field, the crystallite magnetic moments arrange along the field and the FC curve follows the spontaneous magnetization of the material. At the cooling in the absence of the magnetic field, the magnetic moments align along the easy axis of each crystallite, and the sample does not have a total magnetic moment, or the moment is less as compared to the FC mode. Upon applying the field in the heating process, the magnetic moments of the crystallites start to adapt to the field direction what leads to an increase in the total magnetization of the films. However, the spontaneous magnetization of the material begins to decrease with the temperature increase. Thus, competition between these two processes leads to the appearance of a maximum in the ZFC curve.

Though such a picture explains qualitatively the ZFC magnetization temperature behavior, other mechanisms could be attracted to understand this phenomenon, in particular, realization of the spin-glass-like state in ZFC process. In this case,  $T_m$  corresponds to the temperature of the magnetic spins freezing,  $T_f$ . According to the spin glass theory, the  $T_f$  dependence on the value of the magnetic field applied during measurements should be described by a power law  $T_f = a + bH^n$ . For the Ising spin system the exponent  $n = 2/3$ . The analysis of the  $T_m$  dependence on the external magnetic field has shown the regularity (1) implementation in our case with  $n = 2/3$ . Nevertheless, further investigation is necessary to find an adequate mechanism describing the ZFC magnetization temperature dependence.

The typical magnetization curves  $M(H)$  obtained for two co-perpendicular orientations of an external magnetic field relative to the films plane at  $T = 5$  K are shown in figure 4 (left). These are the symmetric hysteresis loops with the close values of the coercive fields  $H_C$  for the both orientations but with different values of the magnetic saturation field  $H_s$  and of different shape. At the perpendicular orientation of the magnetic field, the  $H_s$  value is noticeably higher.

The sharp  $H_C$  decrease and strong change of the loops shape with the temperature decrease from 90 to 5 K are the remarkable features of the films investigated. At  $T = 90$  K, hysteresis, practically, absents; the magnetization curve consists, approximately, of two linear parts with the slope changing at  $H$  value close to  $H_C$  observed at 5 K; magnetic saturation is not reached even in the highest

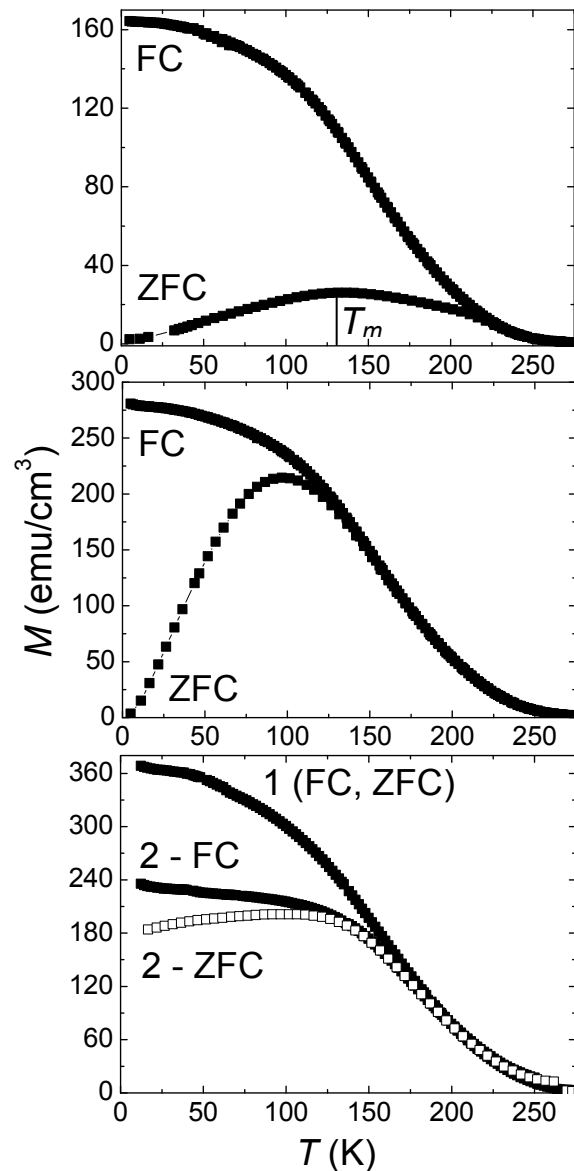


**Figure 3.** FC and ZFC magnetization temperature dependences for the  $\text{Pr}_{0.6}\text{Sr}_{0.4}\text{MnO}_3$  film of 80 nm in thickness, recorded at  $H = 100$  Oe directed in the film plane (top),  $H = 500$  Oe directed in the film plane (in the middle), and  $H = 3$  kOe directed in the film plane (curve 1) and perpendicular to the film plane (curves 2) – bottom.

magnetic field used being of 20 kOe (figure 4 (right)). The absence of magnetic saturation suggests a possible contribution of the Pr spins to the magnetic properties of the samples.

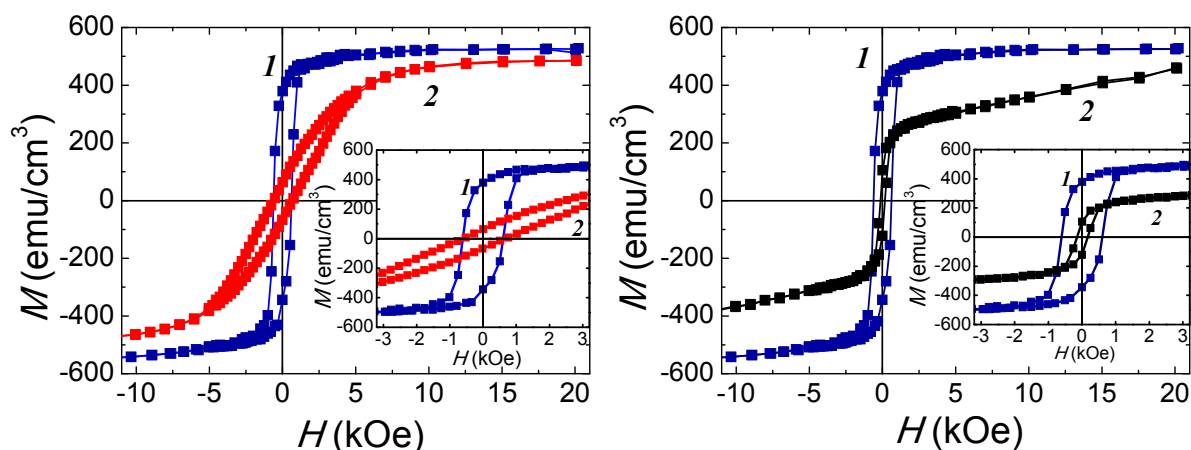


**Figure 4.** Hysteresis loops of the  $\text{Pr}_{0.6}\text{Sr}_{0.4}\text{MnO}_3$  film with thickness of 80 nm: left  $-T = 5$  K, with field  $H$  parallel (curve 1) and perpendicular (curve 2) to the sample plane; right  $-H$  parallel to the sample plane,  $T = 5$  K (curve 1) and  $T = 90$  K (curve 2). The inserts show the same dependences in the region of  $H = \pm 3$  kOe.

The change of the magnetization curves shape with the temperature, in particular, the sharp  $H_C$  decrease when the temperature increases and the hysteresis loop appearance in the perpendicular field can be explained by the effect of the crystallographic anisotropy of the samples. It is known that the manganites crystallographic anisotropy increases approximately by an order of magnitude when the temperature decreases from  $T_C$  to liquid helium temperature [18]. The absence of magnetic saturation at temperatures exceeding  $\sim 25$  K can be associated with the Pr ions effect on the manganite magnetic properties. Indeed, several authors considered a possible coupling between Pr  $4f$  and Mn  $3d$  spins when studying magnetic and transport properties of the praseodymium manganite doped with Pb or Ca [19, 20]. In particular, they found that magnetic ordering in similar compounds was mediated through the indirect exchange between  $4f$  and  $5d$  orbitals which, in turn, was in the direct exchange couplings with the  $3d$  Mn orbitals.

#### 4. Conclusions

We have investigated the structure, resistivity and magnetic properties of  $\text{Pr}_{0.6}\text{Sr}_{0.4}\text{MnO}_3$  polycrystalline films in detail. The resistivity temperature dependence is characteristic for the substances possessing the Mott metal-insulator transition. The magnetization temperature behavior is explained by two mechanisms: an effect of the crystallographic anisotropy and the presence of the spin glass state in the samples arising in the ZFC process. The character of the magnetization field dependences changes essentially with the temperature increase. The hysteresis, practically, disappears at higher temperatures that is associated with a decrease of the crystallographic anisotropy. The magnetic saturation is not reached even in the highest magnetic field used being of 20 kOe that ascribed to the Pr spins contribution to the total magnetization of the films.

#### Acknowledgments

The work was supported partly by RFBR, grant №14-02-01211, Grant of President of Russian Federation №NSh-2886.2014.2, and by The Ministry of Education and Science of the Russian Federation, project №2582.

**References**

- [1] Ramirez AP 1997 *J. Phys.: Condens. Matter.* **9** 8171
- [2] Haghiri-Gosnet A-M, Renard J-P 2003 *J. Phys. D: Appl. Phys.* **36** R127
- [3] Coey J M D, Viret M, von Molnar S 1999 *Adv. in Phys.* **48** 167
- [4] Chmaissem, Dabrowski B, Kolesnik S, Mais J, Jorgensen J D, Short S 2003 *Phys. Rev.B* **67** 094431
- [5] Volkov N V 2012 *Physics-Uspekhi* **55** 250
- [6] Yu-Kuai L, Yue-Wei Y, Xiao-Guang L 2013 *Chin. Phys. B.* **22** 087502
- [7] Boujelben W, Cheikh-Rouhou A, Eellouze M, Joubert J C 2000 *J. Phase Transitions* **71** 127
- [8] Rama N, Sankaranarayanan V, Rao M S 2006 *J. Appl. Phys.* **99** Q315
- [9] Rößler S, Harikrishnan S N, Rößler U K, Kumar C M N, Suja E, Wirth S 2011 *Phys. Rev.B.* **84** 184422
- [10] Repaka D V M, Tripathi T S, Aparnadevi M, Mahendiran R 2012 *J. Appl. Phys.* **112** 123915
- [11] Thaljaoui R, Pekala K, Pekala M, Boujelben W, Szydłowska, Fagnard J-F, Vanderbemden P, Cheikhrouhou A 2013 *J. Alloys Comp.* **580** 137
- [12] Kimura T, Ishihara S, Shintani H, Arima T, Takahashi K T, Ishizaka K, and Tokura Y 2003 *Phys. Rev. B* **68** 060403(R)
- [13] Elleuch F, Triki M, Bekri M, Dhahri E, Hlil E K 2015 *J. Alloys Comp.* **620** 249
- [14] Edelman I, Greben'kova Yu, Sokolov A, Molochev M, Aleksandrovskiy A, Chichkov V, Andreev N, Mukovskii Y 2014 *AIP Advances* **4** 057125
- [15] Mukovskii Y M, Shmatok A V, 1999 *J. Magn. Magn. Matter* **196-197** 136
- [16] Elleuch F, Triki M, Becri M, Dhahri E, and Hlil E K 2015 *J. All. Comp.* **620** 249
- [17] Vencataiah G, Reddy P V 2005 *J. Magn. Magn. Mater.* **285** 343
- [18] Steenbeck K, Hiergeist R, 1999 *Appl. Phys. Lett.* **75** 1778
- [19] Dho J, Kim W S, Chi E O, Hur N H, Park, Ri H-C 2003 *Sol. St. Commun.* **125** 143
- [20] Padmanabhan B, Suja E, Bhat H L, Rößler S, Dörr K, Müller K H 2006 *J. Magn. Magn. Matter* **307** 288